SAND99-0498C

Development of a Compact Optical-MEMS Scanner With Integrated VCSEL Light Source and Diffractive Optics

Thomas W. Krygowski, David Reyes, M. Steven Rodgers, James H. Smith
Microelectronics Development Laboratory, Sandia National Laboratories

Mial Warren, William Sweatt, Olga Blum-Spahn, Joel R. Wendt, Randy Asbill
Compound Semiconductor Research Laboratories, Sandia National Laboratories

http://www.mdl.sandia.gov/Micromachine

ABSTRACT

In this work the design and initial fabrication results are reported for the components of a compact optical-MEMS laser scanning system. This system integrates a silicon MEMS laser scanner, a Vertical Cavity Surface Emitting Laser (VCSEL) and passive optical components. The MEMS scanner and VCSEL are mounted onto a fused silica substrate which serves as an optical interconnect between the devices. Two Diffractive Optical Elements (DOE's) are etched into the fused silica substrate to focus the VCSEL beam and increaase the scan range. The silicon MEMS scanner consists of an actuator that continuously scans the position of a large polysilicon gold-coated shuttle containing a third DOE. Interferometric measurements show that the residual stress in the 500 μm x 1000μm shuttle is extremely low, with a maximum deflection of only 0.18μm over an 800 μm span for an unmetallized case and a deflection of 0.56μm for the metallized case. A conservative estimate for the scan range is ~ $\pm 4^{\circ}$, with a spot size of about 0.5 mm, producing 50 resolvable spots. The basic system architecture, optical and MEMS design is reported in this paper, with an emphasis on the design and fabrication of the silicon MEMS scanner portion of the system.

Keywords: OMEMS, MEMS Scanner, VCSEL, Hybrid Package, Substrate-Mode Architecture, Diffractive Optical Element.

1. INTRODUCTION

Low-speed laser scanning systems, in the range of 10Hz-1kHz can be used in a variety of applications including barcode scanners, video displays, laser print heads, and optical communications. Enabling technologies for compact laser scanning systems are MEMS, optoelectronics and micro-optics. In this work we report on the development of a compact laser scanning system which integrates these three technologies into a compact, manufacturable system. The goal of this paper is to introduce the architecture for this scanner system, and to discuss design and fabrication issues of the silicon MEMS scanner and optical components. Complete system performance data will be reported at a later date. Section 2 of this paper reviews the basic architecture of the integrated scanner system, while Section 3 discusses design and fabrication issues for two generations of the silicon MEMS scanner. Section 4 discusses the design and fabrication of the micro-optical elements, and the conclusion in section 5 reviews the current status and future directions of this compact laser scanning system.

2. SYSTEM ARCHITECTURE

Micromachined scanning mirrors are an ideal choice for a compact laser scanner due to the small size, low power consumption and relative ease of integration with silicon microelectronics. Several groups have demonstrated manipulation of an on-chip laser beam using micromachined components [1,2]. These devices often incorporate manually assembled MEMS prototypes coupled with laser diodes (typically edge-emitting) epoxied to a silicon MEMS substrate. While adequate for demonstration purposes, the assembly costs with this approach are prohibitively high. In the present work, a manufacturable alternative is pursued whereby the (VCSEL) light source and (MEMS) scanner are fabricated separately, and mounted onto a common fused silica substrate which serves as both an optical interconnect between the VCSEL and MEMS and as a component of the hybrid package. This approach, first demonstrated by Jahns and Huang[3], is a way of integrating several optical components onto a single planar substrate for a small inexpensive optical system. To our knowledge, this is the first time this approach has

DISCLAIMER

DISCLAIMER

Portions of this document may be illegible in electronic image products. Images are produced from the best available original document.

been used to integrate free-space micromachinined components with optoelectronic devices. Figure 1 illustrates the basic system architecture.

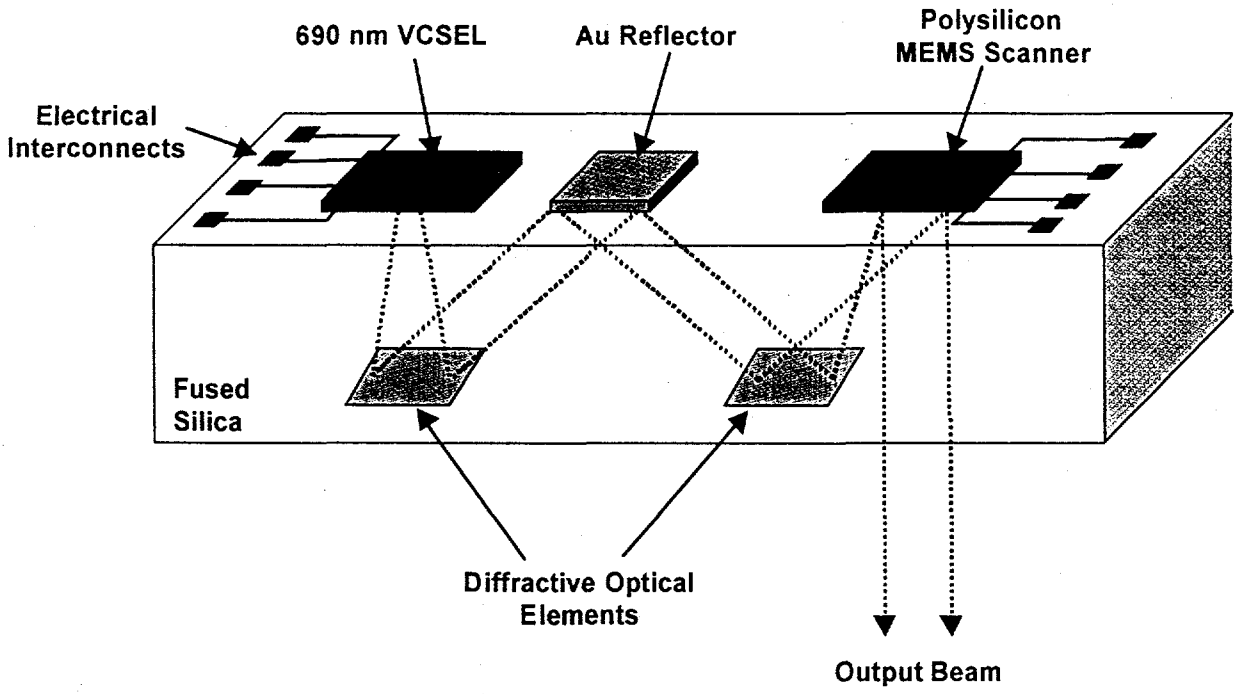

Figure 1. Basic system architecture of MEMS scanner with integrated VCSEL light source. Two DOEs are etched into the fused silica substrate, and a reflector patterned on the surface to direct the VCSEL beam toward the MEMS scanner.

Both the VCSEL and MEMS devices are bonded to the 2mm thick fused silica substrate using a precision alignment flip-chip bonder. Thermocompression bonds around the perimeter of the die form a strong mechanical connection between the die and the fused silica substrate. A portion of the development for this packaging scheme was carried out for the "Chem-Lab-on-a-Chip" project also presented at this conference [4], and has proven to be a reliable method of integrating VCSEL's with other microsystem components. By fabricating the MEMS and VCSEL devices separately, the two components can be optimized. Integration at a later time provides significant design and manufacturing flexibility. In addition, this architecture is scalable, allowing for additional components such as a photodetector or ASIC to be bonded to the fused silica substrate for greater functionality.

Two diffractive optical elements are etched into the fused silica surface to manage the VCSEL beam divergence and to increase the scan range. A diffractive grating is also etched into the polysilicon reflecting surface to collimate the output beam. Further detail on the design and fabrication of the optical components will be discussed below in section 4.

3. MEMS SCANNER DESIGN AND FABRICATION

Most scanning micromirrors fabricated with silicon surface micromachining are designed to be folded out of plane, and rotated about torsion springs or hinges [5,6], as shown schematically in Figure 2. The scan range is typically increased beyond the actuator displacement by relying on the lever arm formed by the close proximity of the torsion hinges to the actuator/mirror connection point. A requirement for the scanning mirror is that the surface of the polysilicon be extremely flat to prevent focussing of the beam which would degrade the resolution of the far field

image. Recent work has shown that corrective optics can be used to partially compensate for curvature of the mirror caused by residual stress gradients in polysilicon[6]. However this would significantly increase the cost and complexity of an integrated laser scanning system. A second requirement is that the mirror must be very rigid to prevent dynamic deformation during operation. The torsion springs must also be made rigid enough to prevent significant translational motion during operation, which in turn requires either a high-force/high-frequency actuator or an actuator that operates at its resonant frequency.

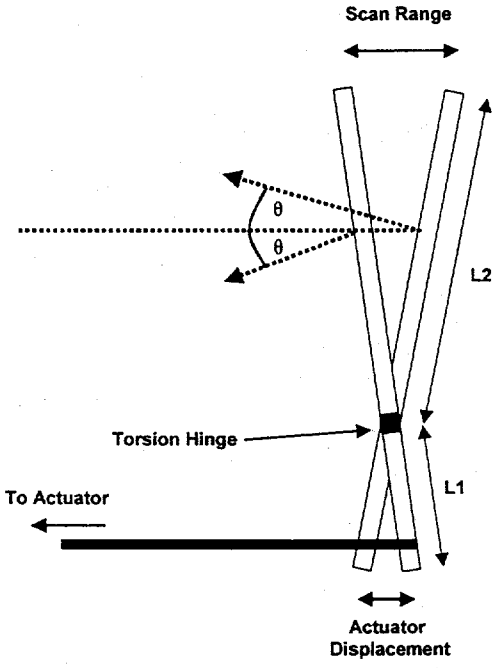

Figure 2. Schematic of typical raster scanning micromirrors using torsion hinges. The scanning range is increased by locating torsion hinges a distance L1 from mirror bottom, where L1<L2.

3.1 First Generation MEMS Scanner

In the present work, an alternative device structure was investigated that would not lead to dynamic bending of the mirror surface and would not require corrective optics or an actuator operating at resonance. The first generation scanner design is shown below in Figure 3. The device was fabricated using Sandia National Laboratories Ultra-planar Multi-level MEMS Technology (SUMMiT), which is a four-level polysilicon MEMS technology available to the public as a foundry service[7]. In the SUMMiT process, the sacrificial oxide below the fourth level of polysilicon is planarized using Chem-Mechanical Polishing (CMP), which removes the underlying topography from the top mirror surface producing a near-optically flat surface. Great care is taken during the SUMMiT fabrication process to reduce intrinsic stress in the mechanical polysilicon layers, and to reduce local roughness. Typical values of local roughness due to polysilicon asparities are on the order of 1-5 nm rms.

The scanner shown in Figure 3 consists of a large 500μm x 1000μm polysilicon shuttle that moves in-plane by a linear rack attached to a rotary actuator. The rotary actuator is a microengine[8], developed at Sandia National Laboratories, consisting of two orthogonal electrostatic comb drives operating 90° out of phase to convert the linear movement of the comb drive to rotational motion. The bondpads and electrical leads to the combdrives were designed with overhanging ridges in the uppermost layer of polysilicon to prevent shorting of the electrical lines during the final blanket evaporation of gold (used to increase the reflectivity of the scanner surface). The microengine is capable of high-speed operation, in excess 100,000 rpm. However, the scanner developed in this work does not require high-speed operation. Thus an additional set of gears was added to serve as a microtransmission[9] with a 12:1 gear reduction ratio. This will reduce the rotational speed by a factor of 12 with a

corresponding increase in torque allowing for greater force to be transmitted to the linear rack and thus overcoming stiction of the large scanning shuttle. The advantage of using a linear rack is that the scan range can be increased by simply increasing the length of the rack and increasing the number of revolutions of the microengine, within the limits of springs attached to the shuttle. The 2 μm wide by 1100 μm long springs on the sides of the shuttle, as shown in Figure 3, are fabricated using three mechanical layers of polysilicon, with a total thickness of 6.75μm, providing out-of-plane rigidity but high in-plane compliance during operation. A conservative estimate for the resonant frequency of the microengine loaded by the mass-spring system of the shuttle is 314 Hz, which is above the intended operating frequency of 100 Hz. During operation, the scanner performed as intended providing smooth operation over the 100 μm scan range, at scan frequencies ranging from 1-100 Hz. However after several hundred cycles the devices tended to fail. The root cause has not yet been identified but wear debris generated by dimples contacting the top surface of the linear rack is proposed as a mechanism for producing discontinuous operation resulting in missed cycles.

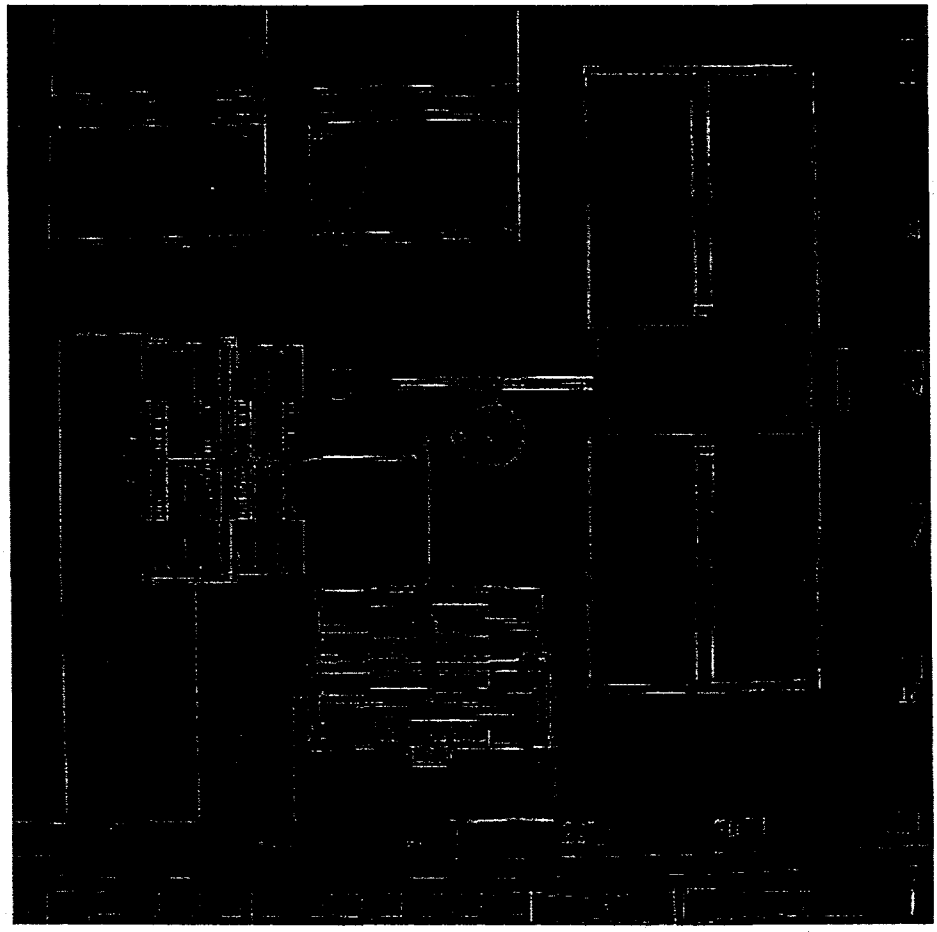

Figure 3. First generation scanner. A large polysilicon shuttle is displaced by a linear rack, which is driven by a microengine/microtransmission assembly.

Fig 4 is an SEM image of the 500μm x 1000μm shuttle (without the diffractive optic) driven by the linear rack, showing the four springs attached to the corners of the shuttle. The large crosses in the corners serve as alignment marks for etching the diffractive optic into the surface of the polysilicon shuttle, and are outside the active area of the lens. Etch release holes were included in the mirror surface to remove the sacrificial oxide underneath. This is not expected to have a dramatic effect on the image quality, since diffraction orders will be outside the area scanned by the output beam. The etch release holes will decrease the efficiency of the device and is estimated to result in a 2% loss. Methods are currently under investigation to remove the sacrificial films from the backside of

the mirror so as to eliminate the need for etch release holes. Once the diffractive optic is etched into the polysilicon shuttle, a 500 Å layer of gold (with a 80 Å Ti adhesion layer) is evaporated onto the surface to improve reflectivity.

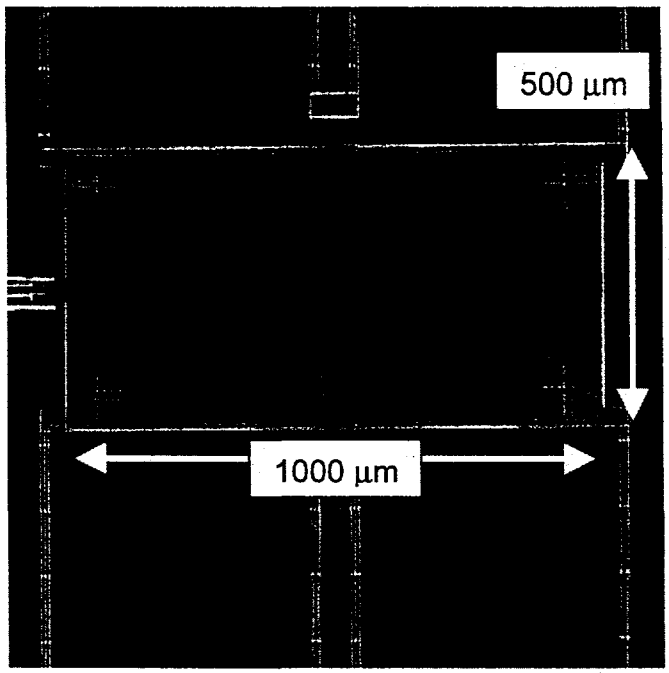

Figure 4. Gold-coated polysilicon shuttle used to manipulate the position of the output of a VCSEL light source.

An important consideration when using large polysilicon structures for optical surfaces is the curvature often found due to residual stress in the polysilicon films. In the case of reflective mirrors used for raster-scanning micromirrors, stress-induced curvature leads to defocussing of the beam, resulting in expansion of the far field image and a loss in resolution. For example, results were recently reported[6] for an unmetallized 250 µm diameter micromirror fabricated at a commercial foundry in which the curvature of the polysilicon film resulted in a center to edge bow of about 1.2 µm. This degree of curvature resulted in a dramatic increase in the far field beam area when compared to a perfectly flat mirror. This problem is usually compounded with the addition of metal on the mirror surface to improve reflectivity.

An effort was made in the present work to achieve as flat a surface as possible by fabricating the shuttle out of three mechanical layers of polysilicon. The total thickness of the polysilicon scanner shuttle is 4.75 µm. To quantify the flatness of this composite structure, z-axis displacement measurements were taken on a released device using a Wyco white light interferometer. The same polysilicon shuttle was measured before and after metallization. The metal coating consisted of an 80 Å Ti adhesion layer, followed by a 500 Å layer of Au, both deposited by e-beam evaporation. The measurements shown in Figure 5a are for line scans along the long axis of the shuttle, while Figure 5b corresponds to line scans along the short axis of the shuttle. The measurements in Figure 5a show a center to edge deflection of only 0.16 um for the unmetallized case over the central 800 µm. This roughly corresponds to the length of the shuttle where the diffractive optic will be etched. After metallization the curvature increased significantly, showing a center to edge deflection of about 0.56 µm over an 800 µm range. Measurements along the short axis of the shuttle in Figure 5b showed a similar trend; the unmetallized case showed essentially no curvature within the measurement limits of the tool, but the metallized case showed a deflection of about of 0.2 µm over a 420 µm span. Based on these measurements it is clear that the as-fabricated polysilicon films are extremely flat, and that most of the curvature in Figure 5 is due to the metal/polysilicon bimorph structure. The impact of etching and metallizing a diffractive optical element into the scanning shuttle can not be determined from these measurements. However, these results do clearly show that the stress level in the 500µm x 1000µm shuttle is extremely low, and

would make an ideal choice in a raster scanning micromirror application. Future efforts will focus on depositing the films in a lower-stress state to further reduce shuttle deflections.

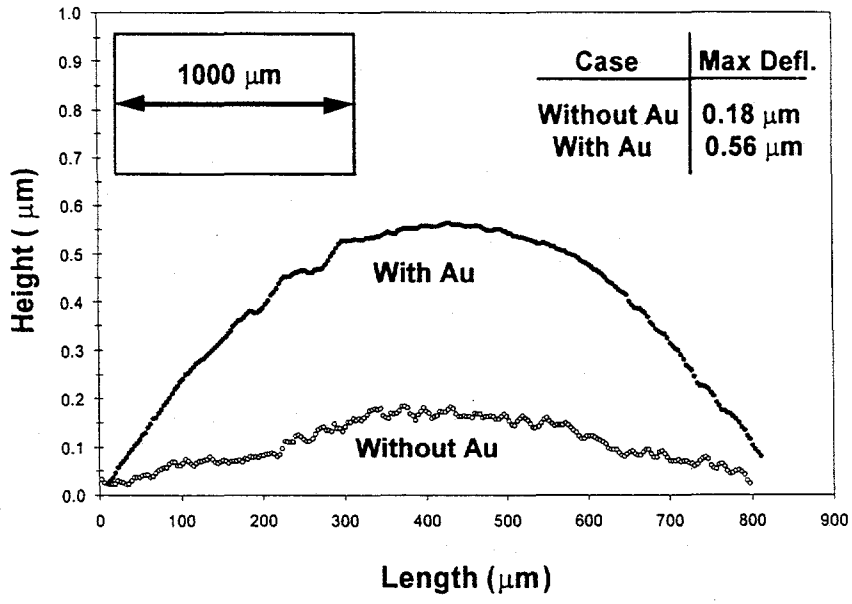

Figure 5a. Inteferometric measurements of z-axis displacement along long axis of large polysilicon shuttle, for cases with and without Au metallization.

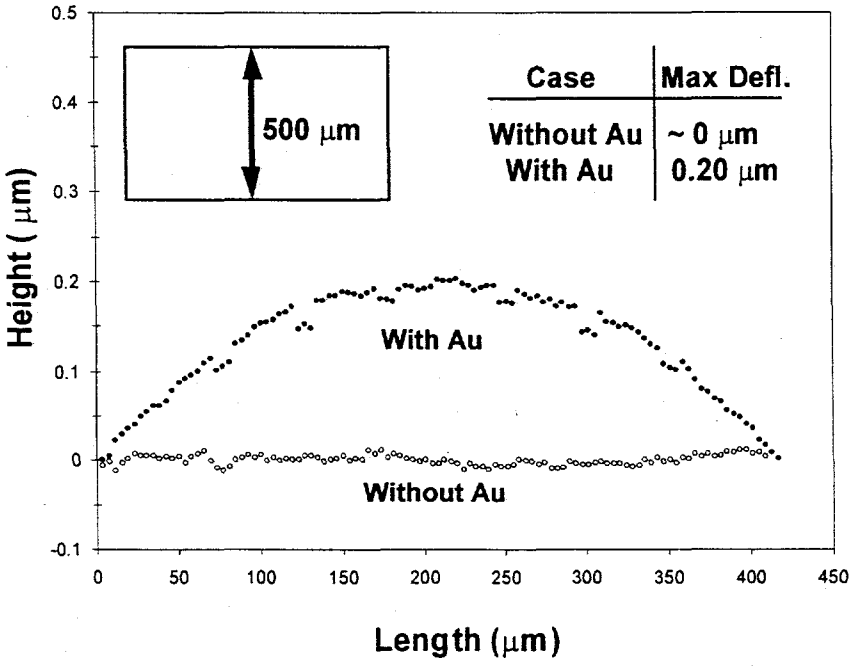

Figure 5b. Inteferometric measurements of z-axis displacement along short axis of large polysilicon shuttle, for cases with and without Au metallization.

3.2 Second Generation MEMS Scanner

As mentioned above, the first generation MEMS scanner had a tendency to fail after several hundred cycles, which is believed to be a result of wear in the linear rack component of the device. A second problem with this device is that the scan range was controlled by a set number of cycles output by the microengine before it reversed direction. If the linear rack briefly jammed while the microengine was running, the scanner would not be displaced the full amount before the microengine reversed direction. Thus, in the second generation scanner a new design was investigated that would allow the actuator to run in a single direction while the shuttle scanned back and forth. Figure 6 shows an SEM image of the second generation scanner. The translation of the shuttle in Figure 6 is controlled by an arm connected to a large output gear from the microengine. As the gear rotates, the arm pushed the scanner shuttle back and forth. In this design the scan range is controlled by the diameter of the gear driving the scanning shuttle, which in this case was designed to give a 100 μm displacement. One point to note in the design in Figure 6 is that a microtransmission was not used. By using an anti-stiction coating after releasing the structures, the high torque generated by the microtransmission was not necessary to drive the 500μm x 1000μm shuttle. Thus the design in Figure 6 is capable of higher speed operation than the previous design, and provides much smoother operation. Work is currently underway to investigate the reliability of this design, but preliminary testing shows that this design is superior by demonstrating much more robust behavior. Future designs will incorporate larger output gears to increase scan range, and a 2D scanner based on the design in Figure 6 is also under development.

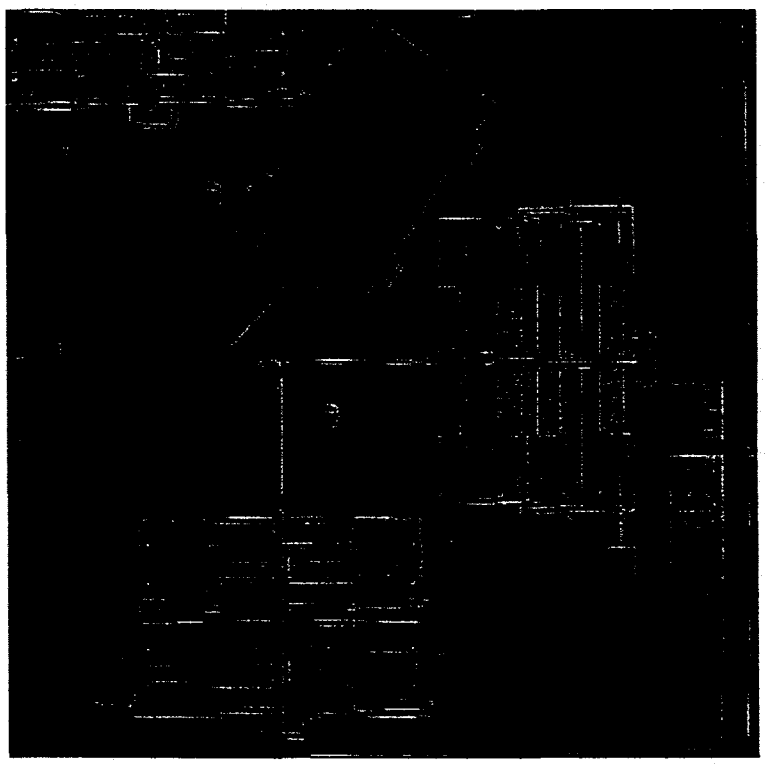

Figure 6. Second generation Optical MEMS scanner using single output gear on microengine.

4. OPTICAL SYSTEM DESIGN AND FABRICATION

The optical system is composed of two diffractive optical elements etched into a fused silica substrate and a third DOE etched into the shuttle of the MEMS scanner. The first two elements relay the beam to the scanner and size it appropriately. The first element collimates the 690-nm VCSEL output beam and tilts it about 20° so there will be room to mount both the VCSEL and the scanner. The second element retilts the beam slightly and focuses it

in front of the third element. The third element, located on the scanner, produces a collimated output beam that is perpendicular to the substrate at the center of the scanner travel.

The system is designed such that the beam is about 500 μm in diameter on all three diffractive elements. Thus the first two elements can be about 600 μm in diameter and the third can be 600 μm by 700 μm. We have chosen to make these binary DOEs with only four phase levels since for this technology demonstration, since fewer processing steps reduces the possibility of damaging the parts. With only four phase levels, the efficiency of each DOE is only 81%. But this is adequate for the intended purpose since $(81\%)^3 > 50\%$. Also, the minimum feature size for the elements is 0.25 μm on the shuttle and slightly larger on the fused silica— this feature size caneasily be written with E-beam lithography.

The diffractive element on the scanner has a focal length of 700 μm and the total travel of the shuttle is 100 μm, therefore, the total scan angle is 0.14 radians which is ±4 degrees or 8 degrees. The optical system is diffraction-limited on axis, and the resulting 0.5 mm spot size is roughly "2x-diffraction limited" at the limits of its $\theta = \pm 4^\circ$ scan range. (Note that the shuttle must move perpendicular to the plane of the paper in Figure 1 or the aberrations will be much larger.)

The four-level diffractive lenses are etched directly into the fused silica substrate and the polysilicon scanner shuttle using Reactive Ion Beam Etching (RIBE), with aluminum as the metal mask. The aluminum mask is first defined using direct-write e-beam lithography. Figure 7 shows a SEM image of test patterns etched into a fused silica substrate. Further details on the fabrication and performance of the optical components of the system will be reported at a later date.

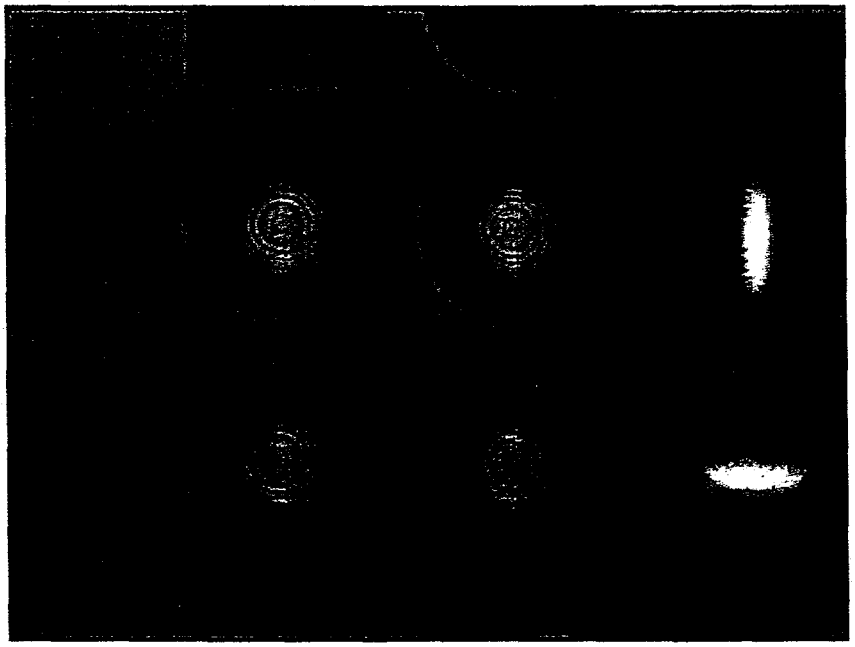

Figure 7. Optical micrograph of an array of on-axis and off-axis lenses fabricated in fused silica.

5. CONCLUSIONS AND FUTURE DIRECTIONS

Preliminary results on the design, fabrication and testing of the components for a compact optical MEMS scanner are presented. The basic system architecture was reviewed for a laser scanning system integrating a VCSEL light source, diffractive optics and a polysilicon MEMS scanner into a compact hybrid package that is believed to be a more manufacturable alternative to previously reported designs. Two generations of MEMS scanners are presented, demonstrating smooth operation at the intended frequency of 100 Hz. Interferometric measurements show that the 500μm x 1000μm scanner shuttle is extremely flat in these designs, with a center to edge deflection of only 0.18 μm over the ~400x900μm^2 active area for the unmetallized case, and 0.56 μm for the metallized case. In the near future results will be reported for the completely integrated laser scanning system.

ACKNOWLEDGEMENTS

The authors would like to thank Mike Russel for the Wyco measurements, Marc Polosky for help in spring design and the members of the Microelectronics Development Laboratories (MDL) and Compound Semiconductor Research Laboratories (CSRL) at Sandia National Laboratories for direct and indirect contributions to this work.

Sandia is a multiprogram laboratory operated by Sandia Corporation, a Lockheed Martin Company, for the United States Department of Energy under Contract DE-AC04-94AL85000.

---

1. M. Ikeda et.al., " Two-Dimensional Silicon Micromachined Optical Scanner Integrated with Photo Detector and Piezoresister", *Transducers 95*, Vol. 1, Stockholm Sweden, pp. 293-296 (1995).
2. M.C. Wu, L.-Y. Lin, S.-S. Lee, K.S.J. Pister, "Micromachined Free-Space Integrated Micro-Optics", *Sensors and Actuators A*, Vol 50, pp. 127-134 (1995).
3. J. Jahns and A. Huang, "Planar Integration of Free Space Optical Components", *Applied Optics*, Vol 28, pp. 1602-1605 (1989).
4. M.E. Warren et.al., "Integrated Micro-Optical Fluorescence Detection System for Microfludic Electrochromatography", *This Conference*, Paper 3878-20, Santa Clara, CA (1999).
5. M.-H Kiang, O Solgaard, R.S. Muller, "Electrostatic Comb-Drive Actuated Micromirrors for Laser Beam Scanning and Positioning" *IEEE J. MEMS*, Vol 7, pp.27-37 (1998).
6. P.M. Hagelin, O. Solgaard, "Optical Raster-Scanning Displays Based in Surface-Micromachined Polysilicon Mirrors", *IEEE J. Selected Topics in Quantum Electronics*, Vol 5, pp. 67-74 (1999).
7. For information about the SUMMiT foundry process, please visit our web site at http://www.mdl.sandia.gov/Micromachine.
8. E. Garcia, J.J. Sniegowski, "Surface Micromachined Microengine", Sensors and Actuators A, Vol 48, pp.203-208 (1995).
9. J. J. Sniegowski, S. M. Miller, G. F. LaVigne, M.S. Rodgers and P. J. McWhorter, "Monolithic Geared-Mechanisms Driven by a Polysilicon Surface-Micromachined On-Chip Electrostatic Microengine", *Solid-State Sensor and Actuator Workshop*, Hilton Head Is., South Carolina, June 2-6, 1996, pp. 178-182.